ELSEVIER

Ceramics International 30 (2004) 585–589

CERAMICS INTERNATIONAL

www.elsevier.com/locate/ceramint

# Dielectric, piezoelectric and pyroelectric properties of PMN–PT (68:32) system

Pawan Kumar [a], Seema Sharma [a], O.P. Thakur [b,*], Chandra Prakash [b], T.C. Goel [a]

[a] *Department of Physics, Indian Institute of Technology, New Delhi-110 016, India*
[b] *Solid State Physics Laboratory, Lucknow Road, Timarpur, Delhi-110 054, India*

Received 20 March 2003; received in revised form 20 May 2003; accepted 3 July 2003

**Abstract**

Solid solution of 32 mol% of Lead Titanate in PMN–PT system has been prepared by columbite precursor method. Room temperature X-ray diffraction study reveals the formation of perovskite phase with tetragonal structure. Dielectric measurements have been carried out at different frequencies (0.1 kHz–1 MHz) as a function of temperature (RT to 235 °C). The phase transition was found to be of diffused type. The polarization studies show ferroelectric nature of the material with a high value of remnant polarization ($P_r$) ~21 μC/cm$^2$ and spontaneous polarization ($P_s$) ~29 μC/cm$^2$. Strain versus electric field (*S*–*E*) behavior shows piezoelectric nature of the material with high value of maximum strain 0.14% at 60 kV/cm. Pyroelectric coefficient at room temperature has been found to be $3 \times 10^{-2}$ μC/cm$^2$ K.
© 2003 Elsevier Ltd and Techna Group S.r.l. All rights reserved.

*Keywords:* C. Dielectric properties; D. Perovskite; Diffuse phase transition; Relaxor

## 1. Introduction

Lead Magnesium Niobate (PMN), a prototype relaxor ferroelectric, demonstrates diffuse phase transition phenomena and around 10 °C a quite high dielectric constant (≅20,000) [1]. The high value of dielectric constant, good voltage stability, excellent electrostrictive effects and lower sintering temperature of PMN make it important for multilayer capacitors, actuators and electro-optic device applications [2,3]. With $PbTiO_3$ (PT), PMN forms a binary solution, (1 − *x*)PMN–*x*PT, and the transition temperature of the system increases with the increase in mol% of PT (Lead Titanate) in the system [3]. 0.9PMN–0.1PT is a pronounced candidate to replace Barium Titanate (BT) in multilayer ceramic capacitors because of its low sintering temperature as well as higher dielectric constant at room temperature than that of BT. This system also has a morphotropic phase boundary (MPB) between 0.70PMN–0.30PT and 0.65PMN–0.35PT compositions. The compositions near MPB of PMN–PT system exhibit excellent piezoelectric properties, thus making the material important for actuator and sensor applications [2]. It has also been reported that compositions near MPB of this system are showing good pyroelectric behavior [4] but not much has been reported on both the pyro- and piezoelectric properties of the same composition [5].

Here, the PMN–PT (68:32) composition is prepared by columbite precursor method and a systematic study of dielectric, piezoelectric, pyroelectric and electromechanical properties of PMN–PT (68:32) composition has been presented.

## 2. Experimental

Polycrystalline samples of PMN–PT (68:32) were prepared by high temperature solid-state reaction via columbite technique [6]. The starting materials were of oxide chemicals with purity better than 99% (all Aldrich). MgO and $Nb_2O_5$ powders were ball milled in distilled water for 8 h using $ZrO_2$ balls as grinding medium. The slurry was dried by heating at 80 °C on a hot plate with continuous stirring. The dried powder was crushed in an agate mortar and calcined in platinum crucible at 1200 °C for 4 h. This columbite ($MgNb_2O_6$) was then crushed and sieved and the powder was again recalcined for 4 h at 950 °C. $TiO_2$ and 4 wt.% excess PbO were mixed with columbite in stoichiometric

* Corresponding author.
*E-mail address:* omprakasht@hotmail.com (O.P. Thakur).

0272-8842/$30.00 © 2003 Elsevier Ltd and Techna Group S.r.l. All rights reserved.
doi:10.1016/j.ceramint.2003.07.003

ratio and ball milled in distilled water using $ZrO_2$ balls. The final calcination was done at 700 °C for 4 h. This calcined powder was again crushed, sieved and mixed with 4 wt.% of polyvinyl alcohol (PVA) binder to impart the mechanical strength to the green pellets. Pellets of 12 mm diameter and 1.25 mm thickness were pressed with an applied pressure of 10 t using uniaxial press. Binder was removed from the green pellets by slowly heating the pellets up to 600 °C and then holding for 1 h. The pellets were then sintered at 1250 °C for 4 h [7]. The electrical contacts were made by coating silver paint on the flat surfaces of the sintered and ground pellets.

X-ray diffraction (XRD) of the pellets was performed on PW 3020 Philips type diffractometer using Cu Kα radiation. Dielectric constant ($\varepsilon_r$) and dielectric loss (tan $\delta$) were calculated from the capacitance measurements using 4284A HP LCR meter at different frequencies (0.1 kHz–1 MHz) as a function of temperature (RT to 235 °C). Using Sawyer Tower circuit, hysteresis (*P–E*) loop was taken with computer interfaced Loop Tracer. The piezoelectric and electromechanical parameters were measured in accordance with the 1961 IRE standards on piezoelectric crystals [8]. Strain versus electric field (*S–E*) behavior was taken using SS-50 Strain Measurement System (Sensor Tec. Ltd., Canada). The samples were poled under corona discharge by applying electric field of 6 kV for 0.5 h. The pyroelectric coefficient was determined by measuring pyroelectric current (*I*) using Keithley electrometer at a heating rate of 4 °C/min. The pyroelectric coefficient ($p_i$) was determined using the relation: $p_i = (I/A)(dT/dt)^{-1}$, where $I$ is the pyroelectric current (measured after repetition of three cycles), $A$ is the electroded area and $dT/dt$ is the heating rate.

## 3. Results and discussion

Fig. 1 shows the room temperature XRD pattern of the sintered sample. The diffraction pattern shows the intense lines of perovskite phase. These diffraction lines were indexed in different crystal systems and unit cell configurations using a computer program package 'Powdmult'. Out of these a suitable tetragonal unit cell was selected for which $\sum \Delta d (= d_{obs} - d_{cal})$, where '$d$' is inter-planer spacing, was found to be minimum. The lattice parameters of the unit cell were refined using least square fit method. The lattice parameters '$a$' and '$c$' are 3.9882 and 4.0549 Å, respectively, with $c/a$, 1.016, and are in agreement with earlier reports [9]. By using the relation [6]

$$\text{Pyrochlore}\,\% = \left[\frac{I_{pyro}}{(I_{perov} + I_{pyro})}\right] \times 100,$$

pyrochlore phase was found to be ~15%.

SEM photograph is illustrated in Fig. 2. It is found that some grains are well developed up to the size of about 2 μm (calculated by linear intercept method). A number of grains

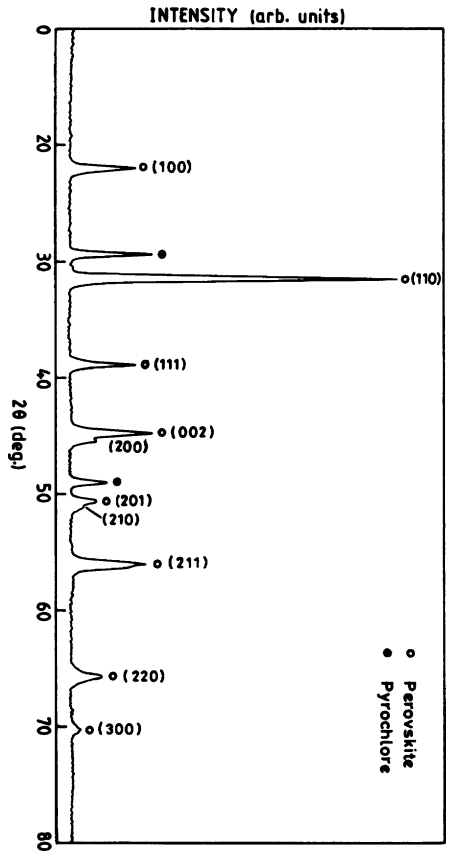


Fig. 1. XRD of the sintered 0.68PMN–0.32PT.

and their grain boundaries are visible, along with a few pores situated upon the grain boundaries.

Fig. 3 shows the variation of dielectric constant ($\varepsilon_r$) with temperature at different frequencies (0.1 kHz–1 MHz). There is a gradual increase in dielectric constant up to 150 °C and this can be attributed to the dominance of interfacial polarization over dipolar polarization [10]. Strong dielectric dispersion without any relaxor behavior has been observed around 190 °C. The strong dispersion in dielectric constant

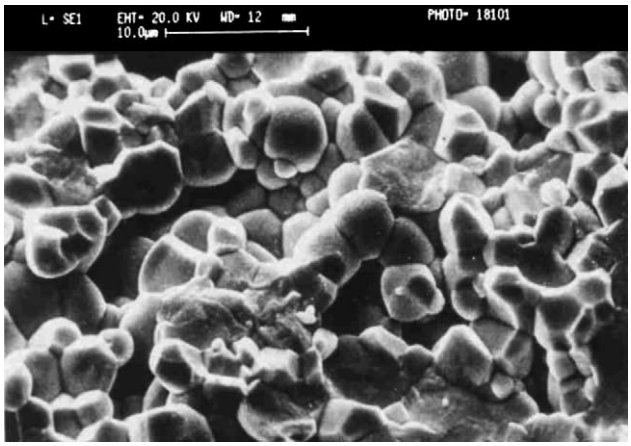


Fig. 2. SEM of the sintered 0.68PMN–0.32PT.

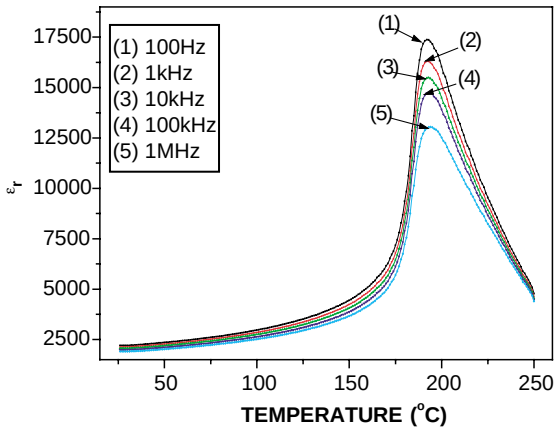


Fig. 3. Temperature dependence of dielectric constant ($\varepsilon_r$) with temperature at different frequencies.

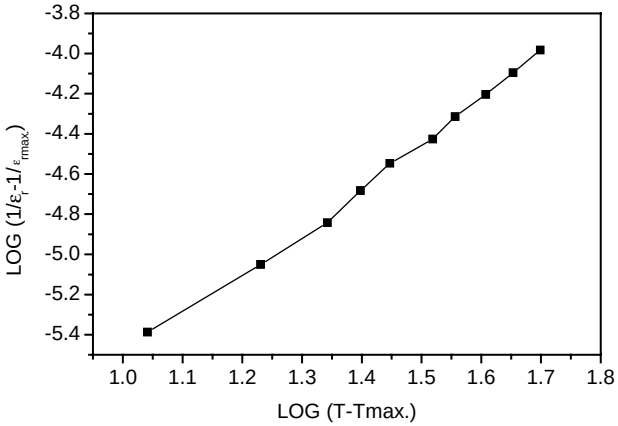


Fig. 5. Variation of $\log(1/\varepsilon_r - 1/\varepsilon_{r\,max.})$ vs. $\log(T - T_{max})$.

near phase transition temperature (Curie temperature) can be due to a Debye-type hopping of defects or impurities over a distribution of barriers. This can also be accounted due to the possibility of marginally softening of lattice mode, which on softening interacts increasingly with the defects and produce a frequency dependent relaxation [11]. Absence of relaxor behavior may be due to the large mol% of PT in the system.

Fig. 4 shows the temperature variation of $\tan\delta$ at different frequencies (0.1 kHz–1 MHz). The temperatures of peak dielectric loss and peak dielectric constant do not coincide up to 100 kHz frequencies. Kramers–Kronig relation indicates that this can be the consequence of temperature dependent relaxation near Curie temperature [11].

The nature of phase transition is ascertained by calculating the degree of diffusion ($\gamma$). Fitting $\varepsilon_r$ at $T > T_{max}$ in formula [12]

$$\varepsilon_r^{-1}(T) = \frac{1}{\varepsilon_{r\,max.}} + (T - T_{max})^{\gamma},$$

a graph between $\log(1/\varepsilon_r - 1/\varepsilon_{r\,max.})$ versus $\log(T - T_{max})$, shown in Fig. 5, is plotted. From the slope of the graph value of '$\gamma$' is calculated. Value of $\gamma$ is found to be ~2, which suggests that the phase transition is of diffused type [12]. The diffuse phase transition in the material may be due to the structural disorder and compositional fluctuations in solid solution. The value of $\varepsilon_r$ and $\tan\delta$ at room temperature and transition temperature at 1 kHz are 2000, 0.025 and 16,500, 0.040, respectively.

Fig. 6 shows the polarization versus electric field ($P$–$E$) behavior of 0.68PMN–0.32PT sample. This figure shows that the material has good ferroelectric nature with $P_s \sim 29\,\mu C/cm^2$ and $P_r \sim 21\,\mu C/cm^2$, which are quite high as compared to previous reported values [13]. At the maximum applied field of 19 kV/cm, coercive field, $E_c$, is found to be ~8.77 kV/cm. The high value of $E_c$ as compared to earlier reported ones [14] can be due to smaller grain size of the material [15].

The piezoelectric charge coefficient ($d_{33}$), and the planar electromechanical coupling coefficient ($k_p$) are found to be 325 pC/N and 40%, respectively. These values are found to be similar with the earlier reports ($d_{33} \sim 410$ pC/N and $k_p \sim 30\%$) [5]. Piezoelectric voltage constant ($g_{33}$), calculated using the relation $g_{33} = d_{33}/\varepsilon_0\varepsilon_r$, is found to be 7 Vm/N.

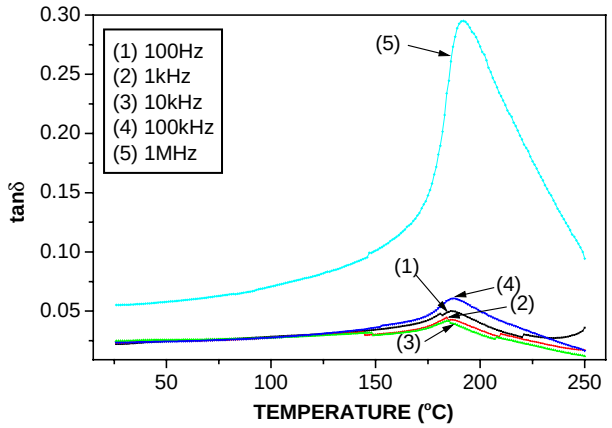


Fig. 4. Temperature dependence of dissipation factor ($\tan\delta$) with temperature at different frequencies.

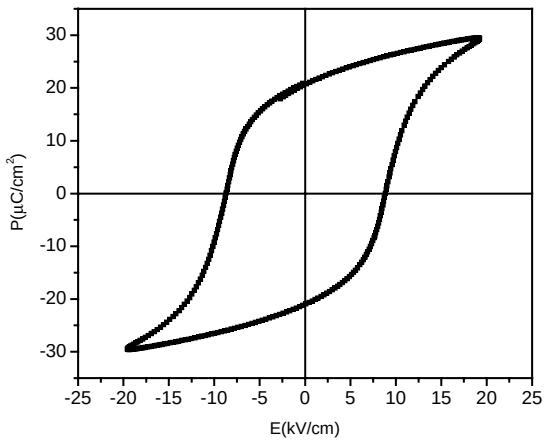


Fig. 6. Variation of polarization vs. electric field.

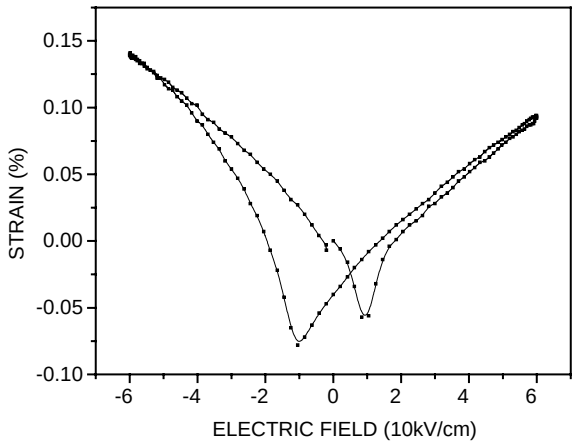


Fig. 7. Variation of strain with biaxial electric field.

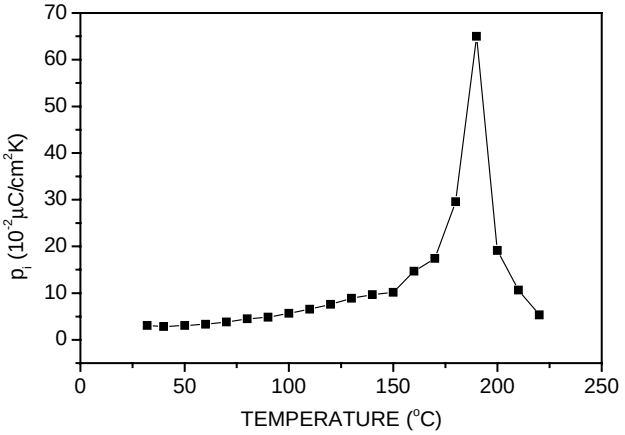


Fig. 9. Variation of pyroelectric coefficient with temperature.

The hysteresis plots between strain and electric field (*S–E*) at room temperature with biaxial and uniaxial fields are illustrated in Figs. 7 and 8. A typical butterfly loop, which is a feature of piezoelectric system is observed for biaxial field. A maximum strain of 0.14 and 0.18% is observed for biaxial and uniaxial fields, respectively. The saturation of strain in both cases was found around 60 kV/cm. The hysteresis observed is due to the polarization reorientation [16] and confirms the piezoelectric nature. However, pure PMN, being electrostrictive, does not exhibit strain hysteresis.

The temperature variation of the pyroelectric coefficient, $p_i$, is shown in Fig. 9. The room temperature value of pyroelectric coefficient is $3 \times 10^{-2}$ μC/cm$^2$ K and it increases with the rise in temperature. The peak value of '$p_i$' is $65 \times 10^{-2}$ μC/cm$^2$ K which is slightly less than the earlier reports ($\sim 100 \times 10^{-2}$ μC/cm$^2$ K) [5]. The peak position is found to be same in both pyroelectric coefficient and dielectric behavior plots taken with the variation of temperature, that confirms the phase transition is around 190 °C. Pyroelectric figures of merit was calculated using specific heat 2.5 J/cm$^3$ K and is listed in Table 1.

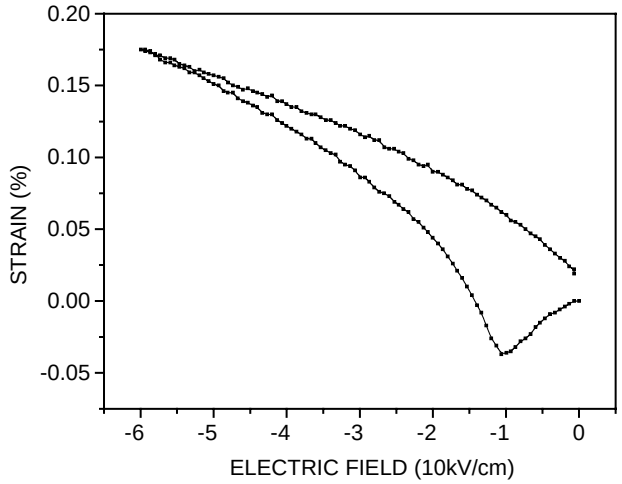


Fig. 8. Variation of strain with uniaxial electric field.

Table 1
Pyroelectric figures of merits of the PMN–PT (68:32) composition at RT

| | |
|---|---|
| Pyroelectric coefficient, $p_i$ (μC/cm$^2$ K) | $3 \times 10^{-2}$ |
| Voltage figure of merit, $F_v$ (V/cm$^2$ J) | 69.60 |
| Current figure of merit, $F_i$ (nA cm/W) | 12.32 |
| Materials figure of merit, $F_D$ (cm$^3$/J)$^{1/2}$ | 0.0059 |

## 4. Summary

PMN–PT (68:32) system reveals perovskite phase with tetragonal structure. It exhibits good ferroelectric characteristics with a diffuse phase transition behavior. Addition of PT in PMN near the vicinity of MPB makes the material piezoelectric, which can be used for high power applications. High value of strain of this material can be exploited in actuator applications while pyroelectric properties can be used for bolometer applications.

## References

[1] L.E. Cross, Ferroelectrics 76 (1987) 241.
[2] T.R. Shrout, J. Fielding Jr., Ultrason. Symp. (1990) 711.
[3] G.H. Haertling, J. Am. Ceram. Soc. 82 (1999) 797.
[4] J.-H. Park, B.-K. Kim, K.-H. Song, S.J. Park, Mater. Res. Bull. 30 (1995) 435.
[5] G.B. Kim, S.W. Choi, Jpn. J. Appl. Phys. 39 (2000) 5552.
[6] S.L. Swartz, T.R. Shrout, Mater. Res. Bull. 17 (1982) 1245.
[7] Y.H. Chen, S. Hirose, D. Viehland, S. Takahashi, K. Uchino, Jpn. J. Appl. Phys. 39 (2000) 4443.
[8] B. Jaffe, W. Cook, H. Jaffe, Piezoelectric Ceramics, Academic Press, London, 1971.
[9] D.H. Suh, D.H. Lee, N.K. Kim, J. Eur. Ceram. Soc. 22 (2000) 219.
[10] L.L. Hench, J.K. West, Principles of Electronic Ceramics, Wiley, New York, 1990.

[11] M.E. Lines, A.M. Glass, Principles and Applications of Ferroelectrics and Related Materials, Clarendon Press, Oxford, 1977.
[12] M. Kuwabara, S. Takahashi, K. Goda, K. Watande, Jpn. J. Appl. Phys. 31 (1992) 3241.
[13] L.B. Kong, J. Ma, W. Zhu, O.K. Tan, Mater. Res. Bull. 37 (2002) 459.
[14] L.B. Kong, J. Ma, W. Zhu, O.K. Tan, J. Alloys Compd. 336 (2002) 242.
[15] C. Sakaki, B.L. Newalkar, S. Komarneni, K. Uchino, Jpn. J. Appl. Phys. 40 (2001) 6907.
[16] K. Uchino, Ferroelectric Devices, Marcel Dekker, New York, 2000.